15TH IEA HEAT PUMP CONFERENCE
MAY 26–29, 2026 | HOFBURG
VIENNA 2026
DECARBONISATION THROUGH INNOVATION

# Investigation of resonant dynamics in elastocaloric systems for energy-efficient cooling

Het Mevada[a], Boyang Liu[b], Ichiro Takeuchi[b], Yunho Hwang[a*]

[a]Center for Environmental Energy Engineering, Department of Mechanical Engineering, University of Maryland, College Park, Maryland, 20742, United States
[d]epartment of Materials Science and Engineering, University of Maryland, College Park, Maryland, 20742, United States
*Corresponding author: Tel: (301) 405-5247, E-mail: yhhwang@umd.edu

## Abstract

Elastocaloric cooling systems, based on the reversible phase transformation of shape memory alloys, offer significant environmental benefits over vapor-compression system by utilizing solid-state refrigerants zero global warming potential and enabling lower energy consumption, thereby contributing to decarbonization efforts. However, the high mechanical work input required for actuation of phase transformation limits the coefficient of performance (COP) and remains a barrier to widespread adoption. This study investigates the dynamic operation of an elastocaloric cooling system under resonant conditions to reduce the actuation work. A single NiTi was cyclically tested to determine the mechanical parameters necessary for resonant frequency and to validate the numerical model. A numerical framework was developed for dynamically operated two NiTi tube bundles operating 180° out-of-phase in reciprocating configuration. Simulation results demonstrate a significant reduction in the input work compared to quasi-static operation, alongside a temperature lift of 32 K and a dynamic amplification factor of 2.9. A sustained cooling performance of 195 W at a temperature lift of 5 K with source and sink temperatures of 20 °C and 25 °C, achieved a maximum COP of 13. Dynamic analysis confirms that resonance-driven operation minimizes energy losses due to mechanical damping, highlighting the potential of resonance tuning as an effective strategy for improving the energy efficiency and viability of elastocaloric cooling technologies.



*Keywords:elastocaloric; numerical modeling; resonance; shape memory alloy*

## 1. Introduction

The rapidly growing global demand for refrigeration and air-conditioning has contributed substantially to greenhouse gas emissions, primarily due to the widespread use of high-global warming potential (GWP) refrigerants, such as hydrofluorocarbons. In response, alternative cooling technologies with minimal environmental impact and potentially higher efficiency have gained increasing attention. Among them, elastocaloric cooling has emerged as a promising candidate, offering a zero-GWP solution [1]. Elastocaloric cooling exploits the elastocaloric effect observed in solid-state refrigerants known as shape memory alloys (SMAs) to produce heating and cooling [2]. This effect arises from the latent heat associated with reversible, stress-induced phase transformation between the austenite and martensite phases of SMAs. Among various SMAs, NiTi-based alloys are the most extensively investigated due to their high latent heat, significant temperature change, commercial availability and giant material-level coefficient of performance (COP) [3]. However, their relatively high transformation stress necessitates a large mechanical work input, posing a limitation to further enhancement of system-level COP.

Recent developments in compression-based elastocaloric systems have demonstrated substantial temperature lift and promising cooling capacities [4], [5], [6]. These systems typically operate through cyclic mechanical loading and unloading, coupled with an intermediate heat exchange process [7]. Experimental and numerical studies indicate that increasing the operational cycle frequency enhances the delivered cooling power [8]. Furthermore, operating at the mechanical resonance frequency can significantly reduce the required input work due to dynamic amplification effects, a concept that has been studied for equivalent spring systems [9], but remains largely unexplored for elastocaloric systems. Alternatively, by effectively recovering the kinetic energy of the actuator, enhancement in performance can be realized [10].

The present study aims to identify the resonant frequency of a compression-based SMA tube and to evaluate the consequent improvements in thermomechanical performance. A comprehensive numerical framework is developed to quantify the enhancement in cooling capacity and reduction in input power achieved through resonance-assisted elastocaloric operation.

## 2. Methods

In dynamic analysis, the spring-mass-damper model represents one of the most fundamental mechanical configurations. In this model, the spring characterizes the system's stiffness, the mass embodies its inertial properties, and the damper accounts for energy dissipation through frictional effects [11]. In the Figure 1(a), the SMA is modeled using spring and damper elements, capturing its elastic response and internal energy losses, respectively. The inclusion of an additional mass component, absent in earlier static configurations, introduces an inertial term that enables the tuning of the system's resonant frequency. The concept, schematic and test methodology are inspired by [12], but in this configuration different SMA lengths are considered to study its effects on resonant frequency. The effective stiffness ($k$) of the system can be determined from the equivalent load-displacement curve, as shown in Figure 1(b). The dynamic behavior of this spring-mass-damper system is governed by the balance of moments about pivot point. By applying Newton's second law of motion and assuming a small displacement ($\theta$), the trigonometric functions are linearized such that $\sin(\theta) \approx \theta$. The resulting equation of motion reflects the contribution of mass ($m$) at distance $a$, and damping ($c$) and stiffness ($k$) components at distance $b$, expressed in Eq. (1). In this formulation, $ma^2$ represents the equivalent mass moment of inertia, while terms $cb^2$ and $kb^2$ defines the effective damping and stiffness of the configuration, respectively. The oscillatory nature of the system is highly sensitive to those geometric parameters, $a$ and $b$, offering significant design flexibility for tuning the system's response. Through this configuration the applied torque can be reduced under dynamic operation as compared to static loading, defined by dynamic amplification factor (DAF). In this study, a polycrystalline $Ni_{50.8}Ti_{49.2}$ (at%) tube provided by Confluent Medical Technologies, having an outer diameter of 4.72 mm, an inner diameter of 3.76 mm, and two lengths of 17 mm and 254 mm was employed. Compression of the tube was conducted using a 250 kN hydraulic universal testing machine (810, MTS Systems Corp.).

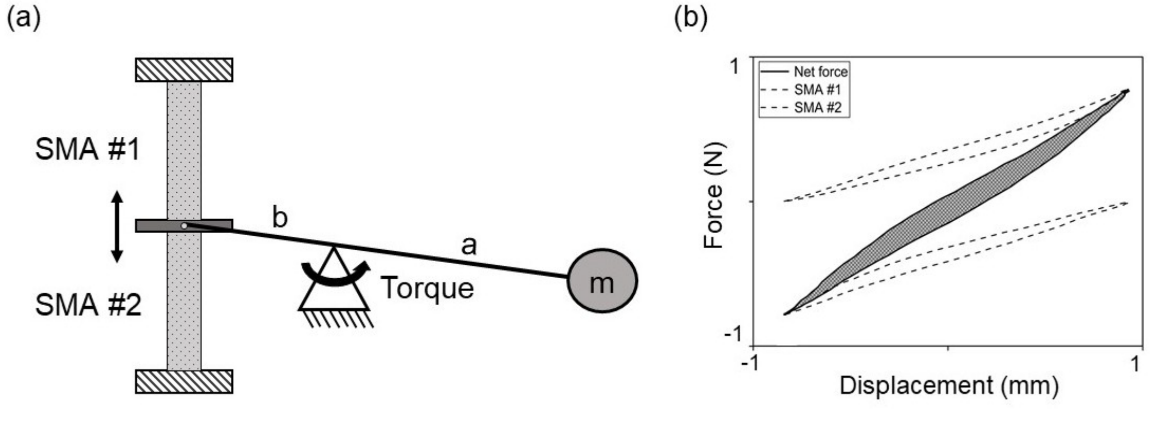


Figure 1. (a) Schematic of two-SMA torque-based system representing equivalent spring-mass-dashpot configuration, with parameters m = 10 kg, b = 0.02 m and a = 1 m. (b) Load-displacement behavior of two-SMA system.

$$T = ma^2\ddot{\theta} + cb^2\dot{\theta} + kb^2\theta \tag{1}$$

Secondly, a numerical model for a dual NiTi regenerator system operating 180° out-of-phase in active regeneration mode was developed using finite element modeling. In active regeneration, the SMA acts as both the primary cooling medium, utilizing latent heat associated with phase transformation and thermal storage matrix for a temperature gradient. By synchronizing the SMA's phase change with the oscillation of a heat transfer fluid (HTF), the system pumps heat across a temperature lift that can be much larger than the material's adiabatic temperature change [13]. The overall framework of the model followed the structure as described in [14]. The utilization factor ($V^* < 1$) is defined as the ratio of the fluid volume displaced through the regenerator during heat exchange period to the total internal fluid volume. This parameter characterizes thermal coupling between the SMA and HTF, directly influencing the regenerator's effectiveness. The design of the simulated system is shown in Figure 2, it consists of two tube bundles, a pump, heat reservoirs, and valves to control flow direction. Each tube bundle consisted of 19 NiTi tubes arranged in hexagonal bundle configuration. The heating and cooling loads were managed by a virtual thermostat based on a PID control algorithm and preset reservoir temperatures. During operation, the two tube bundles functioned in opposite phases, while one was subjected to loading (compression). Both processes were imposed in a sinusoidal manner. The HTF that flowed through each tube bundle was oscillatory and synchronized with the mechanical cycle. The thermomechanical response of the SMA was modeled using the single-crystal kinetic formulation proposed by [7]. Heat exchange between the SMA, the HTF, and other system components was represented through one-dimensional energy balance equations discretized along the tube length. The mass flow rate profile was also assumed to be sinusoidal, reflecting cyclic operation.

The complete system model was implemented in MATLAB Simulink, where the discretized governing equations were solved using ODE15 solver with a relative error tolerance of $10^{-6}$. The system's performance parameters, including temperature lift and cooling power, were evaluated once the system reached steady-state. The temperature lift was defined as the difference between the average temperatures of the hot and cold reservoirs. The mechanical work input to the system was determined by integrating the stress-strain curve, assuming kinetic energy recovery and adding pump work. In out-of-phase tube bundles, the mechanical work released by one bundle during unloading is directly utilized to assist the loading of another bundle. This recovery of kinetic energy minimizes the net external energy input [15]. Finally, the COP of the system was determined as ratio of achieved cooling power to input work, providing a measure of system's dynamic operation performance.

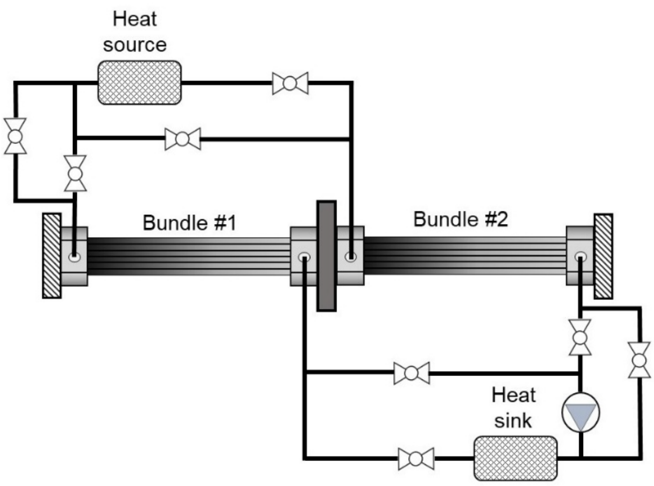


Figure 2. Schematic of two-bundle elastocaloric system with heat sink and heat source.

## 3. Results and Discussion

### *3.1. Experimental validation of natural frequency*

Experimental validation was performed to evaluate the accuracy of the numerical model in predicting the natural frequency of the SMA. The SMA specimens were subjected to dynamic loading and unloading under controlled boundary conditions, with a sinusoidal force applied as the input excitation. The effective spring stiffness ($k$) of each specimen was determined from the ratio of the maximum force to the corresponding maximum displacement, while the damping coefficient was estimated from the slope of the dissipated energy versus displacement-squared curve [16]. Two SMA specimens with lengths of 17 mm and 254 mm were tested, yielding experimental natural frequencies of 8.3 Hz and 2.4 Hz, respectively. These values show good agreement with the numerically predicted frequencies of 8.2 Hz and 2.1 Hz, with a maximum deviation of approximately 12%. The minor discrepancies are primarily attributed to uncertainties in material properties and sensor measurements within the experimental setup. Furthermore, as illustrated in Figure 3, the natural frequency of the SMA exhibits a linear decrease with increasing specimen length when plotted on a log-log scale. This trend highlights a distinct scaling behavior of SMA structures, providing valuable insights for tailoring specimen geometry to achieve desired operating frequency ranges. The strong correspondence between experimental and numerical results confirms the reliability of the developed model in capturing the dynamic response characteristics of the SMA system.

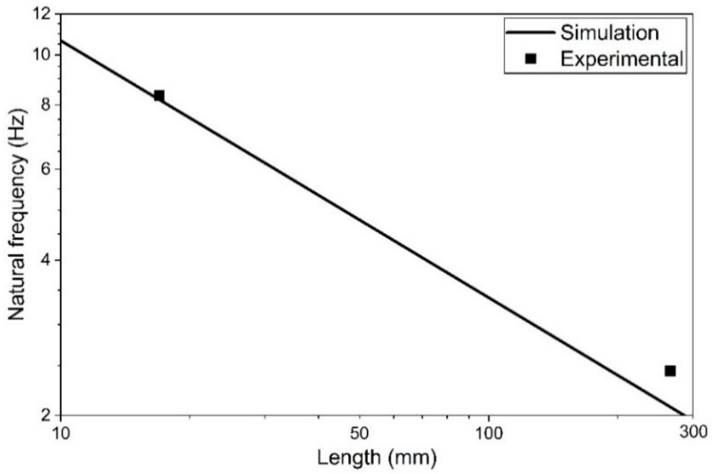


Figure 3. Natural frequency of the SMA tube as a function of length and validation of the numerical model with experimental data.

*3.2. Dynamic simulation and performance of the two-bundle elastocaloric system*

The thermo-mechanical response and overall performance of a two-bundle elastocaloric cooling system were simulated using the numerical framework under dynamic operation. The numerical model incorporated experimentally validated material parameters and boundary conditions to ensure consistency with the results of the SMA specimen. Each SMA bundle was subjected to synchronized sinusoidal excitation, with the variation in displacement and mass flow rate in the tube bundle. There is a phase lag of $2\pi/5$ radian between the displacement and fluid's mass flow rate curve, which ensure that the reverse Brayton cycle is efficiently operated for the elastocaloric system. The maximum mass flow rate is determined based on the cycle frequency and $V^*$.

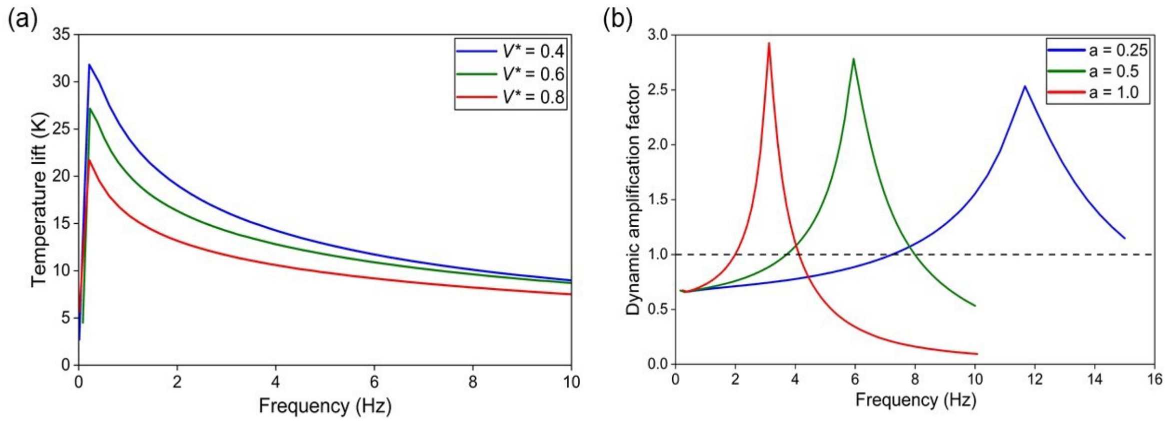


Figure 4. Thermomechanical performance of a two-bundle dynamic elastocaloric system with varying frequency: (a) temperature lift for different $V^*$ values and (b) DAF for different arm lengths.

Figure 4(a) shows the variation in temperature lift of the elastocaloric system as a function of cycle frequency at different $V^*$. The temperature lift was defined at zero cooling load and an input strain of 3.5%. It can be observed that the temperature lift decreases with increasing frequency for all $V^*$. This decline in thermal performance is attributed to the higher thermal time constant of system, which at higher frequency is less efficient for heat transfer. The maximum temperature lift achieved was approximately 32 K at $V^*$ of 0.4, indicating that active regeneration can enhance the temperature lift by a factor of approximately 2.5 compared to the material's adiabatic temperature change. Furthermore, the two-bundle elastocaloric system exhibited a significant reduction in the input torque during dynamic operation relative to static conditions. As shown in Figure 4(b), the system achieves a DAF of 2.9 at a cycle frequency of 3.1 Hz, corresponding to a 65% reduction in maximum torque input at resonance compared to static operation. This demonstrates a substantial improvement in the overall performance of the elastocaloric system.

Additionally, the effect of arm length (*a*) of the attached mass on the DAF was investigated. The results show that decreasing the arm length leads to a hyperbolic increase in the resonant frequency. Specifically, when a was reduced by a factor of four, the resonant frequency increased proportionally from 2.9 Hz to 11.6 Hz. As *a* decreases, the operational range near resonance broadens, indicating a reduction in the system's damping ratio. Consequently, this lower damping results in a sharper torque drop (or higher DAF) near resonance, which can potentially lead to instability during dynamic operation.

The cooling performance of a two-bundle elastocaloric system was numerically evaluated to quantify the potential improvement in COP under dynamic operation. As illustrated in Figure 5(a), the cooling power increases with operating frequency, reaching a peak value of 190 W at 0.8 Hz for $V^*$ of 2. Beyond this point, the cooling power decreases. Across all operating conditions, the source and sink temperatures were maintained at 20 °C and 25 °C resulting in a temperature lift of 5 K. The observed rise and subsequent decline in cooling power with cycle frequency are attributed to the thermal time constants of both the working fluid and SMA. At higher frequencies, these time constants limit effective heat exchange, thereby reducing overall cooling output.

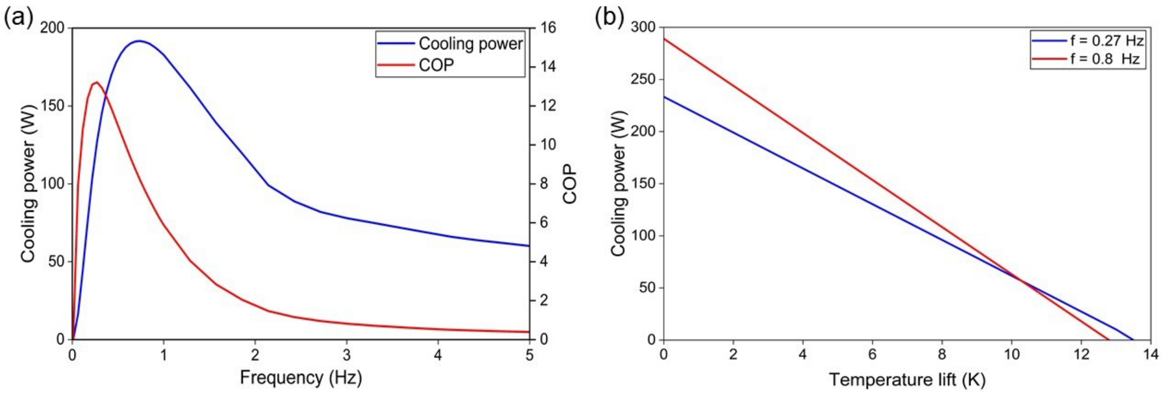


Figure 5. (a) Variation in cooling power and COP with frequency (b) Temperature lift vs cooling power performance at two frequencies.

Dynamic operation significantly influences the mechanical input requirements. Owing to resonance effects, the input torque decreases with increasing frequency, enabling the system to achieve a DAF of 2.7 at 2.9 Hz. However, the average work input continues to increase monotonically because work is proportional not only to torque but also to angular velocity, which scales directly with frequency. As a result, the highest COP of approximately 13 occurs at much lower frequency of 0.27 Hz, where the system benefits from reduces work input despite modest cooling power. These results highlight that elastocaloric cooling systems can strategically exploit resonance to achieve exceptionally high-performance metrics.

The cooling power-temperature lift characteristics were evaluated at operating frequencies of 0.27 Hz and 0.8 Hz. As shown in Figure 5(b), the system operating at 0.8 Hz delivers approximately 20% higher cooling power compared to operation at 0.27 Hz. At 0.8 Hz, the elastocaloric system reaches its maximum cooling capacity, whereas at 0.27 Hz it achieves its maximum COP. This highlights a clear trade-off between cooling performance and system efficiency. However, the difference in optimal operating frequencies remains relatively small, indicating that the dynamic-frequency operation can enable robust, high-performance elastocaloric cooling.

## 4. Conclusions

This study demonstrates that resonant dynamic operation can substantially enhance the performance and energy efficiency of elastocaloric cooling systems. Experimental characterization of NiTi tubes confirmed the predictive accuracy of the developed spring-mass-damper model, with measured natural frequencies aligning closely with numerical results. The validated dynamic model enabled the design and analysis of a two-bundle elastocaloric regenerator configured for out-of-phase operation. The numerical results reveal several key advantages of resonance-assisted operation. First, operating near the resonant frequency significantly reduces mechanical input requirements, with a peak torque reduction of approximately 65% compared to quasi-static loading. At the same time the system achieves a maximum temperature lift around 32 K in active regeneration mode. Secondly, the system maintains high thermodynamic performance under dynamic operation, delivering a maximum cooling power of 190 W at temperature lift of 5 K. The analysis also highlights the inherent trade-off between cooling capacity and COP, governed by the interaction of mechanical resonance, thermal time constants, and flow utilization. Overall, the results confirm that resonance tuning is a powerful strategy for improving the feasibility of elastocaloric technology. By enabling lower input work while preserving strong cooling performance, resonant operation lays the foundation for future high-efficiency elastocaloric heat pumps and refrigeration systems.

**Acknowledgements**

The authors gratefully acknowledge the support of this effort from the National Science Foundation under award number ERC-230175 for the Engineering Research Center EARTH.

**References**

[1] W. Goetzler, R. Zogg, J. Young, and C. Johnson, “Energy savings potential and RD&D opportunities for non-vapor compression HVAC technologies report,” Energy.gov. Accessed: May 25, 2023. [Online]. Available: https://www.energy.gov/eere/buildings/articles/non-vapor-compression-hvac-technologies-report

[2] E. Bonnot, R. Romero, L. Mañosa, E. Vives, and A. Planes, “Elastocaloric Effect Associated with the Martensitic Transition in Shape-Memory Alloys,” *Phys. Rev. Lett.*, vol. 100, no. 12, p. 125901, Mar. 2008, doi: 10.1103/PhysRevLett.100.125901.

[3] S. Qian *et al.*, “A review of elastocaloric cooling: Materials, cycles and system integrations,” *Int. J. Refrig.*, vol. 64, pp. 1–19, Apr. 2016, doi: 10.1016/j.ijrefrig.2015.12.001.

[4] Ž. Ahčin *et al.*, “High-performance cooling and heat pumping based on fatigue-resistant elastocaloric effect in compression,” *Joule*, vol. 6, no. 10, pp. 2338–2357, Oct. 2022, doi: 10.1016/j.joule.2022.08.011.

[5] S. Qian *et al.*, “High-performance multimode elastocaloric cooling system,” *Science*, vol. 380, no. 6646, pp. 722–727, May 2023, doi: 10.1126/science.adg7043.

[6] G. Zhou, L. Zhang, Z. Li, P. Hua, Q. Sun, and S. Yao, “Achieving kilowatt-scale elastocaloric cooling by a multi-cell architecture,” *Nature*, pp. 1–6, Feb. 2025, doi: 10.1038/s41586-024-08549-9.

[7] S. Qian, “Thermodynamics of elastocaloric cooling and heat pump cycles,” *Appl. Therm. Eng.*, vol. 219, p. 119540, Jan. 2023, doi: 10.1016/j.applthermaleng.2022.119540.

[8] Y. Zhu, G. Zhou, S. Cheng, Q. Sun, and S. Yao, “A numerical study of elastocaloric regenerators of tubular structures,” *Appl. Energy*, vol. 339, p. 120990, June 2023, doi: 10.1016/j.apenergy.2023.120990.

[9] S. Unmüßig, A. Burghardt, O. Schäfer-Welsen, and K. Bartholomé, “Highly Efficient Drive System for Elastocaloric Heat Pumps and Cooling Systems,” *Shape Mem. Superelasticity*, vol. 10, no. 2, pp. 177–188, June 2024, doi: 10.1007/s40830-024-00487-9.

[10] S. Yao *et al.*, “Efficient roller-driven elastocaloric refrigerator,” *Nat. Commun.*, vol. 15, no. 1, p. 7203, Aug. 2024, doi: 10.1038/s41467-024-51632-y.

[11] B. Balachandran and E. Magrab, *Vibrations*. in 3rd edition. Cambridge, UK: Cambridge University Press, 2019.

[12] D. Catalini, “Development of Cooling Systems with Active Elastocaloric Regenerators,” Ph.D., University of Maryland, College Park, United States -- Maryland, 2021. Accessed: Mar. 10, 2025. [Online]. Available: https://www.proquest.com/docview/2562786399/abstract/64CE70774F1044C8PQ/1

[13] J. Tušek, K. Engelbrecht, D. Eriksen, S. Dall’Olio, J. Tušek, and N. Pryds, “A regenerative elastocaloric heat pump,” *Nat. Energy*, vol. 1, no. 10, Art. no. 10, Sept. 2016, doi: 10.1038/nenergy.2016.134.

[14] H. Mevada, Y. Hwang, and I. Takeuchi, “Optimization of Heat Transfer Mechanisms in Elastocaloric Cooling Systems,” *Int. J. Refrig.*, 2025, Accessed: Nov. 12, 2025. [Online]. Available: https://www.sciencedirect.com/science/article/pii/S0140700725003743

[15] H. Mevada, B. Liu, L. Gao, Y. Hwang, I. Takeuchi, and R. Radermacher, “Elastocaloric cooling: A pathway towards future cooling technology,” *Int. J. Refrig.*, vol. 162, pp. 86–98, June 2024, doi: 10.1016/j.ijrefrig.2024.03.014.

[16] M. Dolce and D. Cardone, “Mechanical behaviour of shape memory alloys for seismic applications 2. Austenite NiTi wires subjected to tension,” *Int. J. Mech. Sci.*, vol. 43, no. 11, pp. 2657–2677, Nov. 2001, doi: 10.1016/S0020-7403(01)00050-9.